Inorganic Chemistry
Article

Inorg. Chem. **2009**, *48*, 10995–11001 **10995**
DOI: 10.1021/ic9011247

Does Iodate Incorporate into Layered Uranyl Phosphates Under Hydrothermal Conditions?

Jie Ling,[†] Shijun Wu,[†,‡] Fanrong Chen,[‡] Antonio Simonetti,[†] John T. Shafer,[†] and Thomas E. Albrecht-Schmitt*[,†]

[†]*Department of Civil Engineering and Geological Sciences and Department of Chemistry and Biochemistry, University of Notre Dame, Notre Dame, Indiana 46556, and* [‡]*Guangzhou Institute of Geochemistry, Chinese Academy of Sciences, Guangzhou, Guangdong, China 510640*

Received June 10, 2009

Three new layered uranyl phosphates, $Ba_3(UO_2)_2(HPO_4)_2(PO_4)_2$, $Ba(UO_2)F(PO_4)$, and $Cs_2(UO_2)_2(PO_4)_2$, were synthesized under mild hydrothermal conditions. These compounds serve as models for uranium alteration phases that might form when spent nuclear fuel is subjected to oxidizing groundwater containing dissolved phosphate. In order to address the possibility of the incorporation of the key fission product ^{129}I in the form of iodate into uranyl alteration phases, the substitution of IO_3^- for the structurally related $PO_3(OH)^{2-}$ or PO_4^{3-} unit was probed. Iodate incorporation into these phases was investigated using LA-ICP-MS, and these data indicate incorporation of iodine with levels as high as 4162 ppm.

Introduction

A deep understanding of the crystal chemistry of uranium compounds and minerals is motivated in part by their potential impact upon the mobility of radionuclides in a geological repository for nuclear waste and in vadose zones contaminated with actinides.[1] In addition to these important environmental aspects of uranium chemistry, these materials are of substantial fundamental interest because of the rich coordination environments of U(VI) that includes tetragonal, pentagonal, and hexagonal bipyramids.[2] These uranyl polyhedra can link together with each other through different connecting modes such as corner- or edge-sharing. Many oxoanions, such as sulfate,[3] selenate,[4] phosphate,[5] iodate,[6] silicate,[7] and molybdate,[8] have been used as ligands for uranyl cations and result in the formation of various structures containing one-dimensional chains, two-dimensional sheets, or three-dimensional frameworks. These uranium-containing compounds also have several interesting and potentially useful physical and chemical properties, including catalysis,[9] luminescence,[10] and ion-exchange.[11]

*E-mail: talbrec1@nd.edu.

(1) (a) Buck, E. C.; Brown, N. R.; Dietz, N. L. *Environ. Sci. Technol.* **1996**, *30*, 81. (b) Burns, P. C.; Ewing, R. C.; Miller, M. L. *J. Nucl. Mater.* **1997**, *245*, 1. (c) Burns, P. C. *J. Nucl. Mater.* **1999**, *265*, 218. (d) Burns, P. C.; Li, Y. *Am. Mineral.* **2002**, *87*, 550.

(2) Burns, P. C.; Ewing, R. C.; Hawthrone, F. C. *Can. Mineral* **1997**, *35*, 1551.

(3) (a) Doran, M. B.; Norquist, A. J.; O'Hare, D. *Inorg. Chem.* **2003**, *42*, 6989. (b) Doran, M. B.; Cockbain, B. E.; Norquist, A. J.; O'Hare, D. *Dalton Trans.* **2004**, *22*, 3810. (c) Norquist, A. J.; Doran, M. B.; O'Hare, D. *Inorg. Chem.* **2005**, *44*, 3837. (d) Norquist, A. J.; Doran, M. B.; O'Hare, D. *Acta Crystallogr.* **2005**, *E61*, m807. (e) Doran, M. B.; Cockbain, B. E.; O'Hare, D. *Dalton Trans.* **2005**, *10*, 1774.

(4) (a) Krivovichev, S. V.; Kahlenberg, V.; Tananaev, I. G.; Kaindl, R.; Mersdorf, E.; Myasoedov, B. F. *J. Am. Chem. Soc.* **2005**, *127*, 1072. (b) Krivovichev, S. V.; Kahlenberg, V.; Kaindl, R.; Mersdorf, E.; Tananaev, I. G.; Myasoedov, B. F. *Angew. Chem.* **2005**, *44*, 1134. (c) Albrecht-Schmitt, T. E. *Angew. Chem.* **2005**, *44*, 4836.

(5) (a) Danis, J. A.; Runde, W. H.; Scott, B.; Fettinger, J.; Eichhorn, B. *Chem. Commun.* **2001**, *22*, 2378. (b) Doran, M. B.; Stuart, C. L.; Norquist, A. J.; O'Hare, D. *Chem. Mater.* **2004**, *16*, 565. (c) Burns, P. C.; Alexopoulos, C. M.; Hotchkiss, P. J.; Locock, A. J. *Inorg. Chem.* **2004**, *43*, 1816.

(6) (a) Bean, A. C.; Peper, S. M.; Albrecht-Schmitt, T. E. *Chem. Mater.* **2001**, *13*, 1226. (b) Sykora, R. E.; Wells, D. M.; Albrecht-Schmitt, T. E. *Inorg. Chem.* **2002**, *41*, 2304. (c) Shvareva, T. V.; Almond, P. M.; Albrecht-Schmitt, T. E. *J. Solid State Chem.* **2005**, *178*, 499. (d) Ling, J.; Albrecht-Schmitt, T. E. *Inorg. Chem.* **2007**, *46*, 346.

(7) (a) Li, Y.; Burns, P. C. *J. Nucl. Mater.* **2001**, *299*, 219. (b) Wang, X. Q.; Huang, J.; Jacobson, A. J. *J. Am. Chem. Soc.* **2002**, *124*, 15190. (c) Huang, J.; Wang, X. Q.; Jacobson, A. J. *J. Mater. Chem.* **2003**, *13*, 191. (d) Chen, C. S.; Chiang, R. K.; Kao, H. M.; Lii, K. H. *Inorg. Chem.* **2005**, *44*, 3914. (e) Chen, C. S.; Kao, H. M.; Lii, K. H. *Inorg. Chem.* **2005**, *44*, 935.

(8) (a) Krivovichev, S. L; Burns, P. C. *Can. Mineral.* **2001**, *39*, 207. (b) Krivovichev, S. L.; Cahill, C. L.; Burns, P. C. *Inorg. Chem.* **2002**, *41*, 34. (c) Krivovichev, S. L.; Cahill, C. L.; Burns, P. C. *Inorg. Chem.* **2003**, *42*, 2459. (d) Alekseev, E. V.; Krivovichev, S. V.; Malcherek, T.; Depmeier, W. *Inorg. Chem.* **2007**, *46*, 8442.

(9) (a) Hutchins, G. J.; Henegham, C. S.; Hudson, I. D.; Taylor, S. H. *Nature* **1996**, *384*, 341. (b) Dalla Cort, A.; Mandolini, L.; Schiaffino, L. *Chem. Commun.* **2005**, *30*, 3867. (c) Nieweg, J. A.; Lemma, K.; Trewyn, B. G.; Lin, V. S. Y.; Bakac, A. *Inorg. Chem.* **2005**, *44*, 5641. (d) Villiers, C.; Thuery, P.; Ephritikhine, M. *Inorg. Chem. Commun.* **2007**, *10*, 891.

(10) (a) Olken, M. M.; Riagioni, R. N.; Ellis, A. B. *Inorg. Chem.* **1983**, *22*, 2128. (b) Grohol, D.; Clearfiled, A. *J. Am. Chem. Soc.* **1997**, *119*, 4662.

(11) (a) Howe, A. T. *Inorg. Ion Exch. Mater.* **1982**, 133. (b) Pozas-Tormo, R.; Moreno-Real, L.; Martinez-Lara, M.; Rodriguez-Castellon, E. *Can. J. Chem.* **1986**, *64*, 35. (c) Paterson-Beedle, M.; Macaskie, L. E.; Lee, C. H.; Hriljac, J. A.; Jee, K. Y.; Kim, W. H. *Hydromet.* **2006**, *83*, 141. (d) Shvareva, T. Y.; Sullens, T. A.; Shehee, T. C.; Albrecht-Schmitt, T. E. *Inorg. Chem.* **2005**, *44*, 300. (e) Shvareva, T. Y.; Skanthakumar, S.; Soderholm, L.; Clearfield, A.; Albrecht-Schmitt, T. E. *Chem. Mater.* **2007**, *19*, 132. (f) Ok, K. M.; Doran, M. B.; O'Hare, D. *Dalton Trans.* **2007**, *30*, 3325.

Published on Web 10/30/2009

Uranium phosphates have been the subject of special interest for a variety of reasons, one of which is their application in the separation of uranium from other components in spent nuclear fuel because of the relatively low solubility of these compounds.[12] Uranyl phosphates are abundant and structurally rich in natural systems,[13] and their formation subsequently affects the migration (or mobility) of uranium in aqueous systems. Therefore, it is important to study the structure, bonding, stability, and spectroscopic properties of uranium phosphates.

Recently, we discovered the unprecedented intercalation of HIO_3 into the layered hydrated uranyl iodate, $UO_2(IO_3)_2(H_2O)$, to yield $UO_2(IO_3)_2(H_2O)\cdot 2HIO_3$.[6d] This intercalation reaction provides a mechanism by which iodine, in the form of iodate, might be taken up by layered uranyl compounds. ^{129}I is one of the key radionuclides of concern that has been released into the environment as the result of nuclear weapons testing and nuclear power operations, especially at locations like the Hanford Site, Savannah River, Nevada Testing Grounds, and Oak Ridge, and is expected to be one of the primary radionuclides of concern in the proposed repository at Yucca Mountain.[14] ^{129}I is a long-lived ($t_{1/2} = 1.7 \times 10^7$) β-emitter.

In an effort to predict the mechanism for the retardation of the release ^{79}Se from spent nuclear fuel, Chen, Burns, and Ewing analyzed a number of uranyl alteration phases and proposed in which phases anion substitution might take place.[15] The speciation of selenium in water bears some similarities with that of iodine in that the trigonal pyramidal selenite, SeO_3^{2-}, anion exists under oxidizing conditions (along with SeO_4^{2-}), and SeO_3^{2-} has the same basic structure as that of iodate, albeit with a different charge. The principle mechanisms proposed were that the (SeO_3) units could substitute for (SiO_3OH) in phases such as sklodowskite, $Mg[(UO_2)(SiO_3OH)]_2(H_2O)_6$, for ($PO_4$) units in the uranyl phosphates phurcalite $Ca_2[(UO_2)_3(PO_4)_2O_2](H_2O)_7$, as well as the potential for substitution of (SeO_3) for (CO_3) in rutherfordine, $UO_2(CO_3)$. Very recently a report was issued by some of the authors of this present study demonstrating the incorporation of iodine in the form of iodate and metaperiodate into the uranyl silicate, uranophane.[16] In addition, there has been at least one study that indirectly indicates that (SeO_3) can substitute for (CO_3) in rutherfordine $UO_2(CO_3)$.[17] In consideration of the structural similarities between iodate and hydrogen phosphate, $PO_3(OH)^{2-}$, we launched a study on the incorporation of iodate into uranyl phosphate phases.

Herein, we report the preparation, structures, and spectroscopic characterization of three new uranyl phosphate compounds, $Ba_3(UO_2)_2(HPO_4)_2(PO_4)_2$, $Ba(UO_2)F(PO_4)$, and $Cs_2(UO_2)_2(PO_4)_2$. We also probe the incorporation of iodate into these uranyl phosphate phases using laser-ablation inductively coupled plasma mass spectroscopy (LA-ICP-MS).

Experimental Section

Syntheses. $UO_2(NO_3)_2\cdot 6H_2O$ (98%, Alfa-Aesar), H_3PO_4 (85%, Alfa-Aesar), HF (40%, Alfa-Aesar), H_3BO_3(99.99%, Alfa-Aesar), K_2CO_3 (99%, Sigma-Aldrich), Cs_2CO_3 (99.9%, Alfa-Aesar), $BaCO_3$ (99.8%, Alfa-Aesar), and HIO_3 (99.5%, Alfa-Aesar) were used as received without further purification. Distilled and Millipore filtered water with resistance of 18.2 MΩ cm was used in all reactions. PTFE-lined autoclaves were used for all reactions. SEM/EDX analyses were performed using a JEOL JSM-7000F. ***Caution!*** *While the* $UO_2(NO_3)_2\cdot 6H_2O$ *used in this study contained depleted U, standard precautions for handling radioactive materials should be followed. Older sources of uranyl nitrate may not be depleted and enhanced care is warranted for these samples. The HF is extremely hazardous and appropriate skin protection and ventilation is needed.*

$Ba_3(UO_2)_2(HPO_4)_2(PO_4)_2$ (BaUP). BaUP was synthesized by loading $BaCO_3$ (204.2 mg, 1.035 mmol), $UO_2(NO_3)_2\cdot 6H_2O$ (173.1 mg, 0.345 mmol), H_3BO_3 (21.4 mg, 0.345 mmol), H_3PO_4 (0.05 mL, 1.035 mmol), and 0.5 mL of water in a 23 mL PTFE-lined autoclave. The autoclave was sealed and heated at 190 °C in a box furnace. After 4 days, the furnace was cooled to room temperature at a rate of 9 °C/h. The product was washed with water and methanol. Yellow-green crystals were left to dry in the air. Yield: 207.4 mg (90.3% based on U). EDX analysis provided a Ba:U:P ratio of 3:2:4.

$Ba(UO_2)F(PO_4)$ (BaUPF). BaUPF was synthesized by loading $BaCO_3$ (204.2 mg, 1.035 mmol), $UO_2(NO_3)_2\cdot 6H_2O$ (173.1 mg, 0.345 mmol), H_3BO_3 (21.3 mg, 0.345 mmol), H_3PO_4 (0.05 mL, 1.035 mmol), HF (0.1 mL, 2.32 mmol), and 0.5 mL of water in a 23 mL PTFE-lined autoclave. The autoclave was sealed and heated at 190 °C in a box furnace. After 5 days, the furnace was cooled to room temperature at a rate of 9 °C/h. The product was washed with water and methanol and allowed to dry. Yellow crystals of the title compound were isolated as the major product. Yield: 149.4 mg (83.1% based on U). EDX analysis provided a Ba:U:P ratio of 1:1:1. These measurements also confirm the presence of fluoride in the sample.

$Cs_2(UO_2)_2(PO_4)_2$ (CsUP). CsUP was synthesized by loading Cs_2CO_3 (266.3 mg, 0.817 mmol), $UO_2(NO_3)_2\cdot 6H_2O$ (136.8 mg, 0.273 mmol), H_3BO_3 (16.8 mg, 0.272 mmol), H_3PO_4 (0.05 mL, 1.035 mmol), and 0.5 mL of water in a 23 mL PTFE-lined autoclave. The autoclave was sealed and heated at 190 °C in a box furnace. After 5 days, the furnace was cooled to room temperature at a rate of 9 °C/h. The product was washed with water

(12) (a) Benedict, M.; Pigford, T. H.; Levi, H. W. *Nuclear Chemical Engineering*, McGraw-Hill: New York, 1981. (b) Scheetz, B. E.; Agrawal, D. K.; Breval, E.; Roy, R. *Waste Manag.* **1994**, *14*, 489. (c) Hawkins, H. T.; Spearing, D. R.; Veirs, D. K.; Danis, J. A.; Smith, D. M.; Tait, C. D.; Runde, W. H.; Spilde, M. N.; Scheetz, B. E. *Chem. Mater.* **1999**, *11*, 2851.

(13) (a) White, D. E.; Hem, J. D.; Waring, G. A. *Data of Geochemistry*, U.S. Geological Survey: Reston, VA, 1963. (b) Langmuir, D. *Geochim. Cosmochim. Acta* **1978**, *42*, 547. (c) Sandino, A.; Bruno, J. *Geochim. Cosmochim. Acta* **1992**, *56*, 4135.

(14) (a) U.S. Department of Energy. *Viability Assessment of a Repository at Yucca Mountain, Nevada*; Report No. DOE/RW-0508; U.S. Department of Energy, Office of Civilian Radioactive Waste Management: Washington, DC, 1998. (b) Nuclear Regulatory Commission. *NRC Sensitivity and Uncertainty Analyses for a Proposed HLW Repository at Yucca Mountain, Nevada, Using TPA 3.1. Conceptual Models and Data*; Report No. NUREG-1668; U.S. Nuclear Regulatory Commission: Rockville, MD, 1999; Vol. *1*. (c) Nuclear Regulatory Commission. *NRC Sensitivity and Uncertainty Analyses for a Proposed HLW Repository at Yucca Mountain, Nevada, Using TPA 3.1. Results and Conclusions*; Report No. NUREG-1668; U.S. Nuclear Regulatory Commission: Rockville, MD, 1999; Vol. *2*.

(15) Chen, F.; Burns, P. C.; Ewing, R. C. *J. Nucl. Mater.* **1999**, *275*, 81.

(16) Wu, S.; Chen, F.; Kang, M.; Yang, Y.; Dou, S. *Radiochim. Acta* **2009**, *97*, 459.

(17) Albrecht-Schmitt, T. E.; Almond, P. M.; Sykora, R. E. *Inorg. Chem.* **2003**, *42*, 3788.

Table 1. Crystallographic Data for **BaUP**, **BaUPF**, and **CsUP**

compound	**BaUP**	**BaUPF**	**CsUP**
formula mass	1333.93	521.33	995.82
color and habit	yellow-green, prism	yellow, prism	yellow-green, prism
crystal system	monoclinic	monoclinic	orthorhombic
space group	$P2_1/c$ (No. 14)	$P2_1/c$ (No. 14)	*Pbca* (No.61)
a (Å)	9.5055(19)	6.6668(6)	14.1762(11)
b (Å)	8.6987(17)	8.2659(8)	8.9300(7)
c (Å)	10.5439(21)	10.7945(10)	19.5347(15)
β (°)	97.314(4)	92.062(2)	–
V (Å^3)	864.7(3)	594.47(10)	2473.0(3)
Z	2	4	8
T (K)	193	193	296
λ (Å)	0.71073	0.71073	0.71073
maximum 2θ (deg)	56.68	56.58	57.46
ρ_{calcd} (g cm^{-3})	5.115	5.825	5.349
μ(Mo Kα) (cm^{-1})	258.67	340.52	322.75
$R(F)$ for $F_o^2 > 2\sigma(F_o^2)^a$	0.0272	0.0327	0.0438
$R_w(F_o^2)^b$	0.0699	0.0863	0.1284

$^a R(F) = \sum ||F_o| - |F_c|| / \sum |F_o|$. $^b R_w(F_o^2) = [\sum[w(F_o^2 - F_c^2)^2] / \sum wF_o^4]^{1/2}$.

and methanol and allowed to dry. The reaction product contained yellow-green crystals of the title compound as the major product. Yield: 74.4 mg (54.8% based on U). EDX analysis provided a Cs:U:P ratio of 1:1:1.

Crystallographic Studies. Single crystals of $Ba_3(UO_2)_2(HPO_4)_2(PO_4)_2$, $Ba(UO_2)F(PO_4)$, and $Cs_2(UO_2)_2(PO_4)_2$ with dimensions of 0.076 mm × 0.066 mm × 0.021 mm, 0.061 mm × 0.038 mm × 0.036 mm, and 0.088 mm × 0.028 mm × 0.020 mm, respectively, were selected and mounted on glass fibers with epoxy and aligned on a Bruker SMART APEX CCD X-ray diffractometer with a digital camera. Intensity measurements were performed using graphite monochromated Mo Kα radiation from a sealed tube with a monocapillary collimator. The intensities and positions of reflections of a sphere were collected by a combination of 3 sets of exposure frames. Each set had a different φ angle for the crystal, and each exposure covered a range of 0.3° in ω. A total of 1800 frames were collected with an exposure time per frame of 10 s for $Cs_2(UO_2)_2(PO_4)_2$, 30 s for $Ba_3(UO_2)(HPO_4)_2(PO_4)_2$, and 40 s for $Ba(UO_2)F(PO_4)$.

Determination of integrated intensities and global cell refinement were performed with the Bruker SAINT (version 6.02) software package using a narrow-frame integration algorithm. A semiempirical absorption correction was applied using SADABS.[18] The program suite SHELXTL (version 5.1) was used for space group determination (XPREP), direct methods structure solution (XS), and least-squares refinement (XL).[19] The final refinements included anisotropic displacement parameters for all atoms and a secondary extinction parameter. Some crystallographic details are listed in Table 1.

Powder X-ray Diffraction. Powder X-ray diffraction patterns were collected with a Rigaku Miniflex powder X-ray diffractometer using Cu Kα (λ = 1.54056 Å) radiation. The collected patterns were compared with those calculated from single crystal data using ATOMS.[20]

Incorporation of Iodate into Uranyl Phosphates. In order to compare iodate uptake results from crystals grown in the presence of iodate versus those that are added back into iodate solutions, two different experiments were designed as follows: (1) **BaUP**, **BaUPF**, and **CsUP** were synthesized in the presence of HIO_3 and labeled as BaUP1, BaUPF1, and CsUP1. (2) A total of 0.1136, 0.0461, and 0.0905 g of pure **BaUP**, **BaUPF**, and **CsUP** crystals, respectively, were reacted with iodic acid solutions under mild hydrothermal condition (190 °C, 5 days), and labeled as BaUP2, BaUPF2, and CsUP2. The stoichiometric ratios of uranium to iodate in all reactions were kept as 10:1. The prepared crystals were washed several times with hot water and ethanol prior to analysis

Table 2. Selected Bond Distances (Å) for **BaUP**

U(1)–O(1)	2.327(4)	P(1)–O(1)	1.524(4)
U(1)–O(2)	2.409(4)	P(1)–O(2)	1.532(4)
U(1)–O(3)	2.362(4)	P(1)–O(3)	1.535(4)
U(1)–O(4)	2.436(4)	P(1)–O(4)	1.539(5)
U(1)–O(5)	2.278(5)	P(2)–O(5)	1.543(5)
U(1)–O(9)	1.774(4)	P(2)–O(6)	1.598(5)
U(1)–O(10)	1.774(4)	P(2)–O(7)	1.495(5)
		P(2)–O(8)	1.507(5)

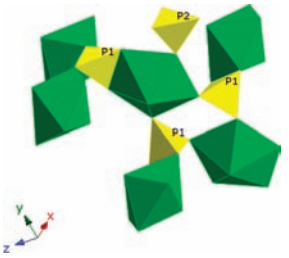

Figure 1. Illustration of the coordination environment of uranium (green) with phosphate ligands (yellow) in $Ba_3(UO_2)_2(HPO_4)_2(PO_4)_2$.

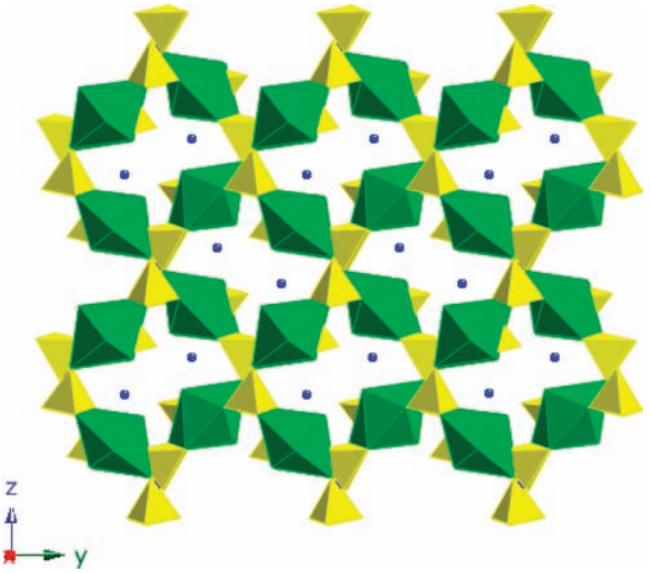

Figure 2. View of a two-dimensional $[(UO_2)_2(HPO_4)_2(PO_4)_2]^{6-}$ layer in $Ba_3(UO_2)_2(HPO_4)_2(PO_4)_2$ that extends in the [*bc*] plane. Uranyl and phosphate are shown as green and yellow polyhedra, respectively. Blue balls stand for barium cations.

(18) (a) Sheldrick, G. M. *SADABS 2001*; Program for absorption correction using SMART CCD based on the method of Blessing. (b) Blessing, R. H. *Acta Crystallogr.* **1995**, *A51*, 33.

(19) Sheldrick, G. M. *SHELXTL PC*, version 6.12; An integrated system for solving, refining, and displaying crystal structures from diffraction data, Siemens Analytical X-Ray Instruments, Inc.: Madison, WI, 2001.

(20) *ATOMS*; version 6.1; Shape Software: Kingsport, TN, 2004.

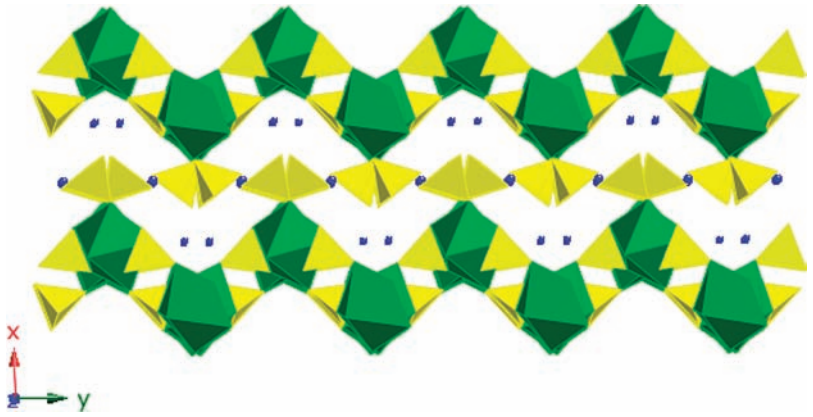

Figure 3. Illustration of the stacking of the $[(UO_2)_2(HPO_4)_2(PO_4)_2]^{6-}$ layers in $Ba_3(UO_2)_2(HPO_4)_2(PO_4)_2$ along the *a* axis. Uranyl and phosphate are shown as green and yellow polyhedra, respectively. Blue balls stand for barium cations.

in an attempt to remove any iodate that might be sorbed on the surfaces of the crystals. These single crystals were then ablated using a New Wave Research UP-213 Nd:YAG laser under a He carrier gas at ~0.710 L/min and an Ar sample gas flow of ~0.9 L/min. The contents of iodine in these crystals were determined by a high-resolution magnetic sector Thermo Finnigan Element 2 inductively coupled plasma mass spectrometer (ICP-MS).

Results and Discussion

Crystal Structure of $Ba_3(UO_2)_2(HPO_4)_2(PO_4)_2$. The title compound contains one crystallographically unique U(VI) center that is strongly bonded to two oxygen atoms, forming a nearly linear UO_2^{2+} cation. The U=O bond lengths within the uranyl cation are 1.774(5) Å (×2) and the O−U−O angle is 176.5(2)°. The UO_2^{2+} cation is further coordinated equatorially by five oxygen atoms and forms a UO_7 pentagonal bipyramid. Within these UO_7 polyhedra, the equatorial U−O bond lengths range from 2.278(5) to 2.436(4) Å. There are also two crystallographically unique phosphorus atoms observed in the structure, and both of them are coordinated by four oxygen atoms in a tetrahedral geometry. The $P(1)O_4^{3-}$ tetrahedron consists of four bridging oxygen atoms bound to three uranyl polyhedra. The P−O bond distances within $P(1)O_4^{3-}$ range from 1.524(5) to 1.539(5) Å. Although P(2) has a similar tetrahedral coordination environment with oxygen atoms, it acts as a terminal ligand and connects to only one uranyl polyhedron. Within the tetrahedron, one oxygen atom is protonated with a P−O(6) bond distance of 1.598(5) Å. The bond distances of the remaining three P−O bonds range from 1.495(5) to 1.543(5) Å. Two crystallographically unique Ba atoms are found in the structure, and both them have 10-coordinate environments. The Ba−O bond distances range widely from 2.642(5) to 3.178(5) Å. The calculated BVS values[21] for U(1),[2] P(1), P(2), Ba(1), and Ba(2) are 6.01, 4.97, 5.11, 2.11 and 2.05, respectively. Selected bond distances are listed in Table 2.

The structure of $Ba_3(UO_2)_2(HPO_4)_2(PO_4)_2$ is of particular interest because it has a new uranyl layered topology. As shown in Figure 1, each uranyl polyhedron is

(21) (a) Brown, I. D.; Altermatt, D. *Acta Crystallogr.* **1985**, *B41*, 244. (b) Brese, N. E.; O'keeffe, M. *Acta Crystallogr.* **1991**, *B47*, 192.

Table 3. Selected Bond Distances (Å) for **BaUPF**

U(1)−O(1)	2.330(6)	P(1)−O(1)	1.545(6)
U(1)−O(2)	2.317(5)	P(1)−O(2)	1.541(6)
U(1)−O(3)	2.398(5)	P(1)−O(3)	1.543(5)
U(1)−O(5)	1.774(5)	P(1)−O(4)	1.509(6)
U(1)−O(6)	1.780(6)		
U(1)−F(1)	2.376(4)		
U(1)−F(1′)	2.394(5)		

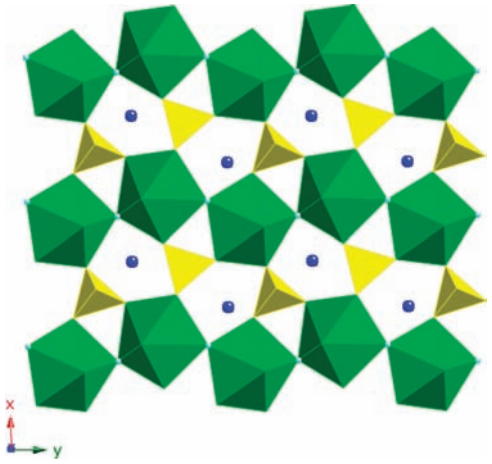

Figure 4. View of the two-dimensional $[(UO_2)F(PO_4)]^{2-}$ layer in $Ba(UO_2)F(PO_4)$ that extends in the [*ab*] plane. Uranyl and phosphate are shown as green and yellow polyhedra, respectively. Blue and light blue balls stand for barium and fluorine atoms, respectively.

coordinated by three bridging $P(1)O_4^{3-}$ tetrahedra and one terminal $HP(2)O_4^{2-}$ tetrahedron. Among these three bridging $P(1)O_4^{3-}$ tetrahedra, one of them is connected to the uranyl polyhedron through edge-sharing and the other two combine to the uranyl polyhedron through corner-sharing. These uranyl polyhedra are joined together through bridging $P(1)O_4^{3-}$ ligands to form a $[(UO_2)_2(HPO_4)_2(PO_4)_2]^{6-}$ layer in the [*bc*] plane with terminal $HP(2)O_4^{2-}$ ligands pointing out of the layer. These anionic layers further stack along the *a* axis and form a layered structure. Ba^{2+} cations, which act as counterions, reside in the interlayer space between adjacent $[(UO_2)_2(HPO_4)_2(PO_4)_2]^{6-}$ layers. A view of the two-dimensional $[(UO_2)_2(HPO_4)_2(PO_4)_2]^{6-}$ layer in $Ba_3(UO_2)_2(HPO_4)_2(PO_4)_2$ that extends in the [*bc*] plane is shown in Figure 2. An illustration of the stacking of the $[(UO_2)_2(HPO_4)_2(PO_4)_2]^{6-}$ layer

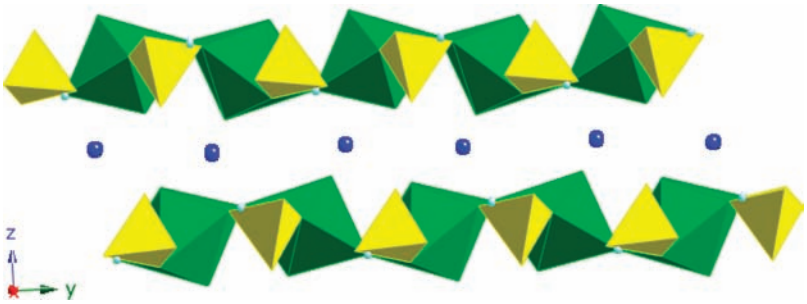

Figure 5. An illustration of the stacking of the $[(UO_2)F(PO_4)]^{2-}$ layers in $Ba(UO_2)F(PO_4)$ along the *c* axis. Uranyl and phosphate are shown as green and yellow polyhedra, respectively. Blue and light blue balls stand for barium and fluorine atoms, respectively.

in $Ba_3(UO_2)_2(HPO_4)_2(PO_4)_2$ along the *a* axis is shown in Figure 3.

Crystal Structure of $Ba(UO_2)F(PO_4)$. In the structure of $Ba(UO_2)F(PO_4)$, there is only one crystallographically unique U(VI) center that exits as a nearly linear UO_2^{2+} cation with U=O bond lengths of 1.774(5) and 1.780 (5) Å, and a O−U−O angle of 175.1(3)°. The uranyl cation is further coordinated by three oxygen atoms and two fluorine atoms in the equatorial plane to form a UO_5F_2 pentagonal bipyramid. The equatorial U−O bond lengths range from 2.317(5) to 2.398(5) Å, and the U−F bond lengths are 2.376(5) and 2.395(5) Å. One distinct phosphorus site and one distinct barium site are observed in the structure. The phosphorus atom is coordinated by four oxygen atoms in a tetrahedral geometry with P−O bond distance ranging from 1.509(6) to 1.545(6) Å. Nine-coordinate Ba^{2+} ions are found interacting with eight oxygen atoms and one fluorine atom. Ba−O bond lengths range from 2.644(6) to 3.183(6) Å, and the Ba−F bond length is 2.791(5) Å. The calculated BVS values[21] for U(1),[2] P(1), and Ba(1) are 6.07, 5.08, and 2.12, respectively. Selected bond distances are listed in Table 3.

The uranyl pentagonal bipyramids are joined together through two corner-sharing fluorine atoms to form a chain extending along the *b* axis. These chains are further linked by tridentate phosphate anions to form a $[(UO_2)F(PO_4)]^{2-}$ layer in the [*ab*] plane. The anionic layer has a similar topology to the $[(UO_2)_2F_2(HPO_4)_2]^{2-}$ sheet in the structure of $[(CH_3)_2NH(CH_2)_2NH(CH_3)_2][(UO_2)_2F_2(HPO_4)_2]$.[22] These anionic layers stack along the *c* axis with barium cations imbedded the interlayer space as counterions. A view of the two-dimensional $[(UO_2)F(PO_4)]^{2-}$ layer in $Ba(UO_2)F(PO_4)$ that extends in the [*ab*] plane is shown in Figure 4. An illustration of the stacking of the $[(UO_2)F(PO_4)]^{2-}$ layers in $Ba(UO_2)F(PO_4)$ along the *c* axis is shown in Figure 5.

Crystal Structure of $Cs_2(UO_2)_2(PO_4)_2$. There are two crystallographically unique U(VI) centers in the structure of $Cs_2(UO_2)_2(PO_4)_2$. The U=O bond lengths are 1.777(9) and 1.78(1) Å in the $U(1)O_2^{2+}$ cation and 1.785(8) Å and 1.79(1) Å in the $U(2)O_2^{2+}$ cation. The O−U−O angles are 176.4(4)° and 177.0(4)°, respectively. Both of the UO_2^{2+} cations are further equatorially coordinated by five oxygen atoms to form UO_7 pentagonal bipyramids in which the equatorial U−O bond lengths range from 2.249(8) to 2.601(8) Å for U(1) and 2.227(8) to 2.584(8) Å for U(2). There are also two crystallographically unique

Table 4. Selected Bond Distances (Å) for **CsUP**

U(1)−O(9)	1.777(9)	U(2)−O(4′)	2.433(8)
U(1)−O(10)	1.78(1)	U(2)−O(7′)	2.226(8)
U(1)−O(2)	2.457(8)	U(2)−O(8′)	2.315(8)
U(1)−O(1)	2.601(8)	P(1)−O(1)	1.548(8)
U(1)−O(1′)	2.427(8)	P(1)−O(2)	1.579(8)
U(1)−O(5)	2.305(8)	P(1)−O(3)	1.485(9)
U(1)−O(6′)	2.249(7)	P(1)−O(4)	1.547(8)
U(2)−O(11)	1.79 (1)	P(2)−O(5)	1.529(8)
U(2)−O(12)	1.783(8)	P(2)−O(6)	1.532(8)
U(2)−O(2)	2.423(8)	P(2)−O(7)	1.550(8)
U(2)−O(4)	2.584(8)	P(2)−O(8)	1.538(8)

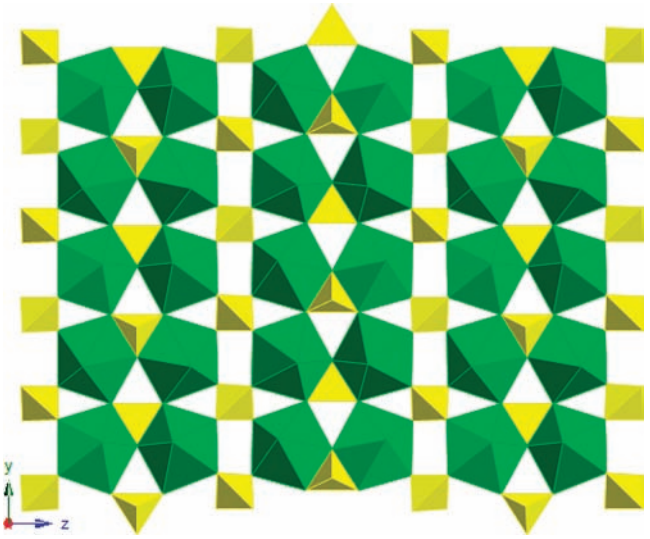

Figure 6. View of the two-dimensional $[(UO_2)_2(PO_4)_2]^{2-}$ layer in $Cs_2(UO_2)_2(PO_4)_2$ that extends in the [*bc*] plane. Uranyl and phosphate are shown as green and yellow polyhedra, respectively.

phosphorus atoms observed in the structure of $Cs_2(UO_2)_2(PO_4)_2$, and both of them are coordinated by four oxygen atoms to form a tetrahedral geometry. The $P(1)O_4^{3-}$ tetrahedron has one terminal oxygen atom with the P−O bond as 1.489(9) Å. The remaining three P−O bond distances within $P(1)O_4^{3-}$ range from 1.547(8) to 1.580(9) Å. Furthermore, the $P(1)O_4^{3-}$ tetrahedron is connected to two uranyl polyhedra via edge-sharing and to another two uranyl polyhedra via corner-sharing. While the $P(2)O_4^{3-}$ tetrahedron consists of four bridging oxygen atoms bound to four uranyl polyhedra, and the P−O bond distances range from 1.530(8) to 1.549(9) Å. Two different Cs^+ cations are observed in $Cs_2(UO_2)_2(PO_4)_2$, and both of them are coordinated by 10 oxygen atoms. The Cs(1)−O and Cs(2)−O bond distances range

(22) Ok, K. M.; Doran, M. B.; O'Hare, D. *Dalton Trans.* **2007**, 3325.

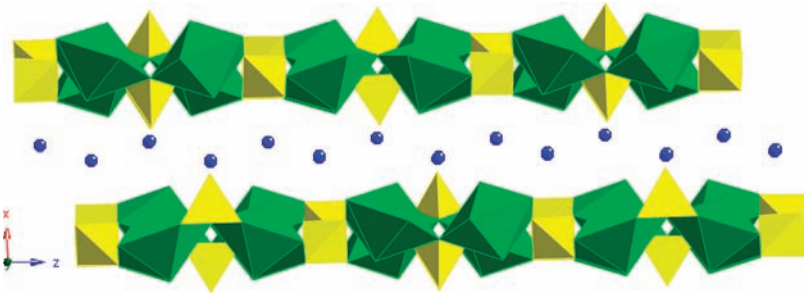

Figure 7. Illustration of the stacking of the $[(UO_2)_2(PO_4)_2]^{2-}$ layers in $Cs_2(UO_2)_2(PO_4)_2$ along the *b* axis. Uranyl and phosphate are shown as green and yellow polyhedra, respectively. Blue balls stand for Cs atoms.

from 2.932(8) to 3.60(1) Å, and 2.930(8) to 3.635(8) Å, respectively. The calculated BVS values[21] for U(1), U(2)[2], P(1), P(2), Cs(1), and Cs(2) are 5.96, 5.95, 4.92, 4.95, 0.98, and 1.13, respectively. Selected bond distances are listed in Table 4.

The structure of $Cs_2(UO_2)_2(PO_4)_2$ also has a new and highly unusual uranyl layered topology. As shown in Figure 6, each of the U(1) or U(2) uranyl polyhedra connects to another two U(1) or U(2) uranyl polyhedra through corner-sharing to form a chain of uranyl polyhedral along the *b* axis. Each U(1) uranyl polyhedra chain also connects to another U(2) uranyl polyhedra chain via corner-sharing along the *c* axis. Between the adjacent U(1) and U(2) polyhedra, there is a $P(1)O_4^{3-}$ tetrahedron. Both of the U(1) and U(2) polyhedra share an edge with the $P(1)O_4^{3-}$ tetrahedron. The terminal P−O bond in the $P(1)O_4^{3-}$ tetrahedra alternately point up and down. The ribbons of uranyl polyhedra are joined together by tetradentate $P(2)O_4^{3-}$ through corner-sharing to form a $[(UO_2)_2(PO_4)_2]^{2-}$ layer in the [*bc*] plane. Cesium cations reside in the interlayer space between two adjacent $[(UO_2)_2(PO_4)_2]^{2-}$ layers. A view of the two-dimensional $[(UO_2)_2(PO_4)_2]^{2-}$ layer in $Cs_2(UO_2)_2(PO_4)_2$ that extends in the [*bc*] plane is shown in Figure 6. An illustration of the stacking of the $[(UO_2)_2(PO_4)_2]^{2-}$ layers in $Cs_2(UO_2)_2(PO_4)_2$ along the *a* axis is shown in Figure 7.

Incorporation of Iodate into Layered Uranyl Phosphates. Iodate-incorporated **BaUP**, **BaUPF**, and **CsUP** single crystals were analyzed using laser-ablation ICP-MS in which single crystals were first ablated by a laser and subsequently analyzed by ICP-MS at a mass of 127. As shown in Figure 8, there is a low and smooth background for the ^{127}I mass before the laser-ablation starts. As soon as the laser shutter opens (start at 60 s), stable peaks of ^{127}I were observed that demonstrate the existence of iodine in the single crystals of **BaUP**, **BaUPF**, and **CsUP**. Table 5 shows the concentration of incorporated iodate in all samples. The average content of iodine in BaUP1, BaUPF1, and CsUP1 are 4162, 2923, and 100 ppm, respectively. It is clear that the iodate uptake values change significantly between these compounds with the highest uptake occurring for the most open layers.

The most likely mechanism for iodate incorporation into these compounds is the substitution of iodate for phosphate, $(IO_3^-) \leftrightarrow (PO_4^{3-})$. Thus, the different coordination of PO_4^{3-} in the structures will result in a different quantity of incorporated iodine. As discussed previously, **BaUP** has two different PO_4^{3-} sites: $P(1)O_4^{3-}$

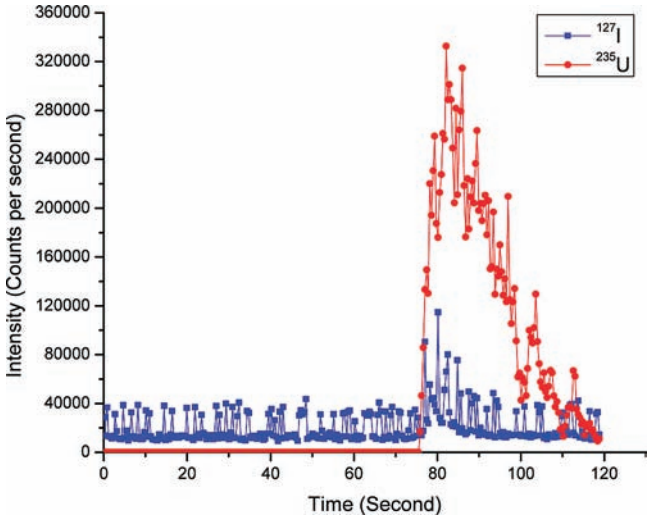

Figure 8. LA-ICP-MS spectrum for ^{127}I and ^{235}U in a typical iodate incorporated $Cs_2(UO_2)_2(PO_4)_2$ single crystal.

is connected to three UO_7 pentagonal bipyramids and $P(2)O_4^{3-}$ is connected to one UO_7 pentagonal bipyramid. It is unlikely that the substitution $IO_3^- \leftrightarrow P(1)O_4^{3-}$ will happen because this will disrupt the structural connectivity. However, $P(2)O_4^{3-}$ is connected to only one UO_7 bipyramid by corner-sharing, which makes it possible for IO_3^- to substitute for PO_4^{3-}, $IO_3^- \leftrightarrow P(2)O_4^{3-}$. With the incorporation of iodate into the structure, an additional charge-balancing mechanism is required to maintain electrostatic neutrality. The most likely possibility is losing some Ba^{2+} cations between the sheets, which can be described as follows

$$Ba_3(UO_2)_2(HPO_4)_2(PO_4)_2 + xIO_3^- \rightarrow$$

$$Ba_{(3-0.5x)}(UO_2)_2(HPO_4)_{(2-x)}(IO_3)_x(PO_4)_2 +$$

$$0.5xBa^{2+} + xHPO_4^{2-} \quad (1)$$

The PO_4^{3-} tetrahedron in **BaUPF** is connected to three UO_5F_2 pentagonal bipyramids, with O···O contacts in the range of 2.473−2.536 Å. This is similar to the O···O contacts of IO_3^- in several uranyl iodates whose O···O distances range from 2.484 Å to 2.793 Å.[6a,d] Because of the small O···O contacts differences between PO_4^{3-} and IO_3^-, it is probable for IO_3^- to substitute for PO_4^{3-} via sharing three oxygen atoms with the UO_5F_2 pentagonal bipyramids, if structural connectivity is not disrupted

Table 5. Iodate Incorporation into Uranyl Phosphate Crystals

sample name	BaUP1	BaUP2	BaUPF1	BaUPF2	CsUP1	CsUP2
concentration of ^{127}I (ppm)	4162	412	2923	1241	100	139

by the elimination of an anion apex due to the substitution.

$$Ba(UO_2)F(PO_4) + xIO_3^- \rightarrow Ba_{(1-x)}(UO_2)F(PO_4)_{(1-x)}(IO_3)_x + xBa^{2+} + xPO_4^{3-} \quad (2)$$

There is a $P(2)O_4^{3-}$ tetrahedron in **CsUP** that is connected to four UO_7 pentagonal bipyramids by corner-sharing. Because of the potential structure disruption, it is unlikely for iodate to substitute for $P(2)O_4^{3-}$. However, the $P(1)O_4^{3-}$ tetrahedron is connected to two uranyl polyhedra via edge-sharing and to another two uranyl polyhedra via corner-sharing, which makes it is possible for $P(1)O_4^{3-}$ to be substituted by IO_3^-. Thus, the mechanism of iodate substitute for PO_4^{3-} in **CsUP** should be similar to that in **BaUPF**.

$$Cs_2(UO_2)_2(P_{(1)}O_4)(P_{(2)}O_4) + xIO_3^- \rightarrow Cs_{2(1-x)}(UO_2)_2(P_{(1)}O_4)_{(1-x)}(IO_3)_x(P_{(2)}O_4) + 2xCs^+ + xP_{(1)}O_4^{3-} \quad (3)$$

By extrapolating from LA-ICP-MS data, substitutions of phosphate become more facile with fewer shared corners or edges in the structure. Thus, the iodate concentration in BaUP1 is higher than BaUPF1. The iodine incorporation abilities before crystal growth and after are different according to different compounds. BaUP1 and BuUPF1, which are grown together with iodate, can uptake much more iodate than BaUP2 and BuUPF2. However, there is no significant difference between CsUP1 and CsUP2.

Conclusions

The question posed in the title of this manuscript has been answered in the affirmative. Iodate can indeed be incorporated at significant levels into the structures of uranyl phosphates that form under mild hydrothermal conditions. This indicates that iodate also can be incorporated into some natural uranyl phosphate minerals such as phurcalite, $Ca_2[(UO_2)_3(PO_4)_2O_2](H_2O)_7$. Therefore, the mobility of ^{129}I in geologic repositories can be reduced significantly through this mechanism.

Acknowledgment. We are grateful for support provided by the Office of Civilian Radioactive Waste Management, Office of Science and Technology and International, through a subcontract with Argonne National Laboratory.

Supporting Information Available: X-ray crystallographic files for $Ba_3(UO_2)_2(HPO_4)_2(PO_4)_2$, $Ba(UO_2)F(PO_4)$, and $Cs_2(UO_2)_2(PO_4)_2$. This material is available free of charge via the Internet at http://pubs.acs.org.